ACS OMEGA

http://pubs.acs.org/journal/acsodf

Article

Minimizing the Barite Scale in Carbonate Formations during the Filter Cake Removal Process

Jaber Al Jaberi, Abdulmalek Ahmed, Badr Bageri,* Mahmoud Elsayed, Mohamed Mahmoud, Shirish Patil, Karem Al-Garadi, and Assad Barri

Cite This: *ACS Omega* 2022, 7, 17976−17983

Read Online

ACCESS | Metrics & More | Article Recommendations

ABSTRACT: The barite scale is one of the most common scales in the oil and gas industry. It can form in the reservoir or precipitate in different production equipment. The formation of such a scale will significantly minimize the capillary diameter of the flow channels and consequently shrink the well productivity. On the other hand, the production of movable barite particles causes severe erosion for the installed equipment. There are several sources of the barite scale such as mixing of incompatible brines and solid invasion of the barite weighted during drilling. In addition, the barite scale could be produced during the interaction of the chelating agent solutions with the reservoir formation during the filter cake removal process (secondary damage). The main focus of this study is to prevent the barite scale inside the carbonate formations during filter cake removal. The capability of a solution consisting of both diethylenetriamine pentaacetic acid (DTPA) and ethylenediamine tetraacetic acid (EDTA) as a novel solution to prevent barite scale formation in carbonate formations after the removal of the barite filter cake was evaluated. A series of laboratory experiments were accomplished to characterize the barite scale and evaluate the performance of the proposed solution. In particular, particle size distribution, scanning electron microscopy, X-ray diffraction, core flooding, NMR spectroscopy, solubility test, and inductively coupled plasma (ICP) spectroscopy tests were conducted for this aim. The experiments were performed using carbonate core samples. The results showed that the proposed solution was able to load 35 000 ppm barium in the presence of calcite ions. The addition of EDTA tended to inhibit the barite deposition and improve the rate of the calcite reaction. NMR results showed that a mixture of DTPA and EDTA (20%) can stimulate the macropores, resulting in an increase in the return permeability by 1.4−1.8 times of the initial value, while the precipitation that occurred in the micropores could be ignored with respect to the overall porosity improvements.

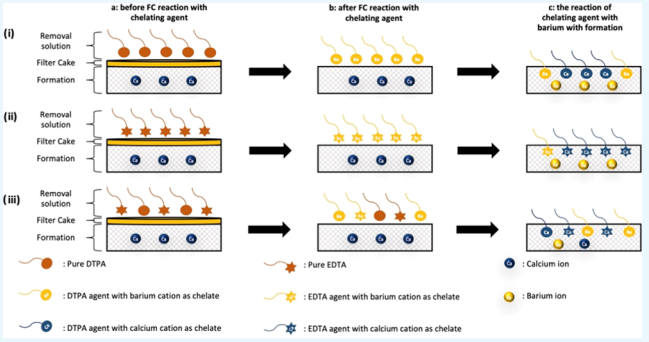

1. INTRODUCTION

Barite ($BaSO_4$) is an inorganic and insoluble salt that has many applications in many fields. In its pure form, it is colorless and has a rhombic crystal shape. Around 80% of the barite in the world is utilized for drilling operations in the petroleum industry.[1,2] It is commonly used as the weighting agent for drilling deep oil and gas wells.[3−6] The reasons behind this are low production cost and its high specific gravity. Accordingly, it is the primary source of the solids in the filter cake when used as a weighting material.[7−9] The other source of the solids in the filter cake is the small fine drilled cutting that integrated with drilling fluid compression and affected the filter cake properties.[10−13] In overbalance drilling operation, there is a need for high specific gravity to suppress the downhole pressure especially for deep gas and oil wells.[14] The mud filter cake will form due to the pressure gradient and with the possibility of invasion into the formation.[15] This could cause the barite to precipitate as a scale in the near-wellbore area, which decreases the productivity and can cause erosion to the chokes and valves if the production operation started without addressing the scale problem.[16,17] These problems have a substantial economic impact, and that is why millions of dollars are paid every year to remove barite from the formation.

Removing the barite scale is not a trivial task mechanically or chemically, especially since barite has low solubility in water.[18] Also, it has low solubility in common acids such as formic acid, lactic acid, citric acid, and hydrochloric acid (HCl).[18,19] Chelating agents are chemicals with many applications in different industries.[20−24] They were introduced as an efficient

Received: March 6, 2022
Accepted: April 28, 2022
Published: May 19, 2022

https://doi.org/10.1021/acsomega.2c01339
ACS Omega 2022, 7, 17976−17983

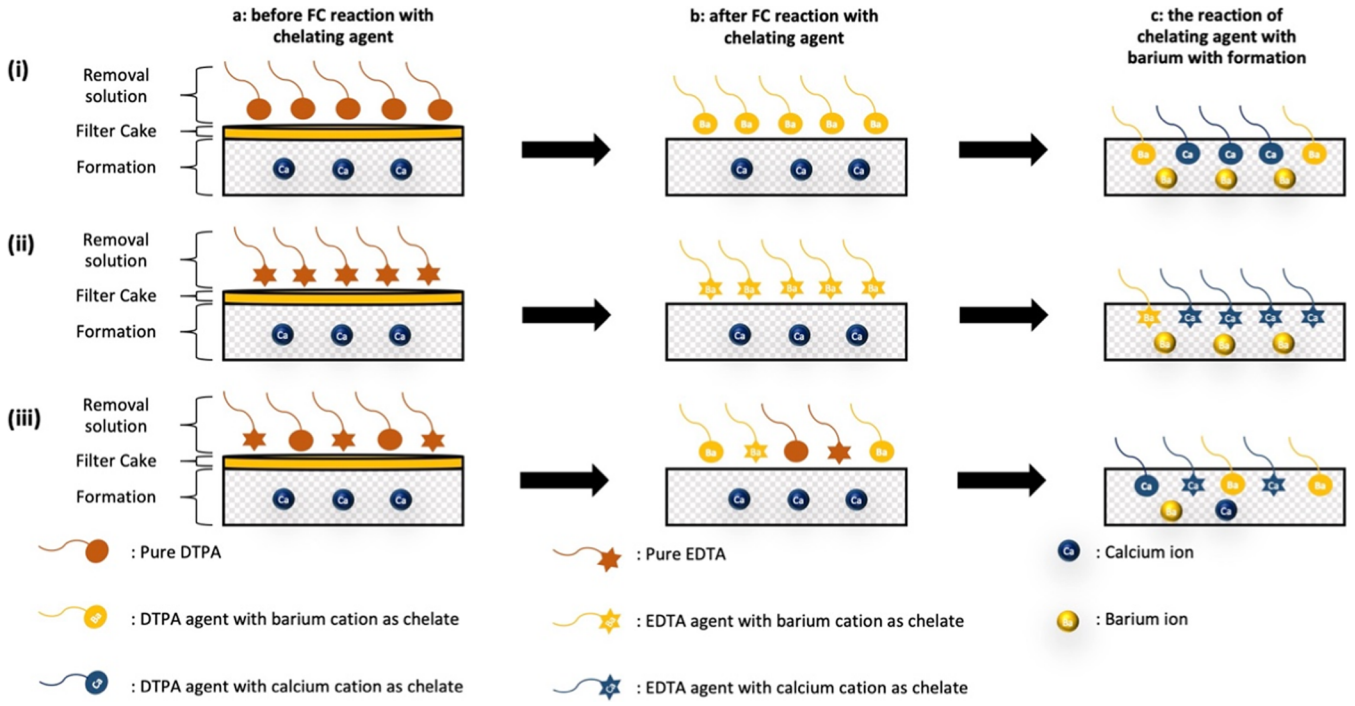

Figure 1. Mechanism of the proposed solution.

barite dissolver.[19,25] Different chelating agents were tested including DTPA, EDTA, HEDTA, DOCTA, NTA, and TTHA to dissolve barite (i.e., Table A1 shows the full name of each chelating agent).[26] The DTPA was found to be one of the most efficient in dissolving the barite scale. Other chelates such as EDTPO have a higher stability constant compared to that of DTPA, but the preparation difficulties and the high cost compared to those of DTPA make it an unfavorable choice.[27] Converting agents were introduced to improve the reaction rate, which was found to have a profound impact on the performance of the chelating agents. Bageri et al.[18,28−30] and Mahmoud et al.[3,31] introduced the use of catalytic conversion for barite dissolution. Catalysts such as potassium carbonate, potassium chloride, potassium hydroxide, cesium carbonate, and cesium formate were introduced to enhance barite scale dissolution. The barite scale dissolution rate increased from 60 wt % to more than 90 wt % after the introduction of catalysts into DTPA. They reached an optimum formulation of 20 wt % DTPA + 6 wt % catalyst for optimum barite scale removal. Improving the dissolver performance required a deep understanding of the reasons and mechanisms of barite scale formation.

The causes for the barite scale formation can be attributed to different mechanisms depending on the source of the barium or barite. It could originally exist in the formation as barium or in the formation brine with excess barium ions.[32] On the other hand, it could be introduced into the formation during the different operations such as the injection and drilling operations. From the injection operation perspective, the barite scale can form when seawater (high sulfate content) is injected in a formation containing barium ions due to the chemical incompatibility. In addition, the mixing of brine from different sources such as multiple zones or wells (specifically the one with a high sulfate content) can cause barite formation.[9,10] In the drilling operations, using barite as weighting materials can cause mud filtrate invasion, which leads to the formation of a mud cake that comprises mainly barite. Moreover, some barite particles may invade the formation to precipitate in the pores, causing a permeability reduction.[7,8]

Another possibility of the barite scale is the secondary damage, which can be formed during the barite filter cake removal process as a result of the interaction between the removal solvents with the formation. Bageri et al.[33,34] illustrate the significant of such a problem, with reduction in the new porosity for the sandstone formation. Even through there was an increase in the overall porosity in the carbonate samples, the large pores were plugged by the dropped barium from the removal solution. They showed how the metallic ions on the formation surface can affect the secondary damage process. Abdelgawad et al.[35] showed that the existence of calcium carbonate has a highly negative impact on the solubility of barite in the DTPA. Moreover, the removal process of the barite filter cake can also cause a deep invasion of the removal solution (which is saturated with barium) into the formation, resulting in a barite scale deposition deeper in the reservoir.[36] Therefore, there is a need for practical solution to minimize the secondary damage phenomenon.

Previous work of filter cake removal did not consider the competitive reaction between the filter cake removers and the solids in both the filter cake and formation. The remover can dissolve the filter cake and may invade the formation; in this case, it will react with the formation rocks. Calcite has a high affinity for reaction with barite removers; in this case, the barium-based scales may precipitate in the formation due to the high reactivity of calcite with the remover.

The objective of this study is to introduce a solution that can prevent barite scale deposition as a secondary damage during the filter cake removal process where the filter cake removal solution is saturated with barium from the filter cake with an abundant amount of calcium carbonate in the formation (i.e., carbonate reservoirs). A solution of diethylenetriamine penta-

https://doi.org/10.1021/acsomega.2c01339
ACS Omega 2022, 7, 17976−17983

acetic (DTPA) acid and ethylenediamine tetraacetic acid (EDTA) was used in this study, which simultaneously stimulates the formation and limits the barite scale formation. The efficiency of the proposed solution was evaluated during the stimulation process of the calcite formation where the proposed solution was injected to stimulate the formation and reacts with calcium carbonate. The industrial barite was characterized by different experiments, while the performance of the proposed solution was evaluated by several experiments. The paper consists of the material and experimental section, which will show the materials used and the experimental procedure. The Results and Discussion section will show the results of each experiment with detailed discussion. Finally, the conclusion will be presented with some recommendations.

2. MATERIALS AND METHODS

The proposed solution mechanism can be explained through Figure 1; it shows the mechanisms of three solutions including using a single chelating agent (i.e., solution (i) and (ii)) or a mixture of chelating agents, which is proposed in this study (solution (iii)). Also, the figure demonstrates the different stages of the interaction between the chelating agent, filter cake, and formation including the stage before the interaction occurs between the chelating agent and filter cake (stage a), the interaction between the chelating agent and filter cake (stage b), and the interaction of the chelating agent with the formation after dissolving the filter cake (stage c). The first solution (i) illustrates the usage of DTPA as a filter cake removal solution; the DTPA dissolves the barite filter cake by the attachment of the chelating ligand to the barium (Ba) site, forming eventually a Ba−DTPA complex.[37] The formed complex, then, comes into contact with the formation rock, which is a carbonate formation in this study. When this occurs, the abundance of calcium cations (Ca^{2+}) in the formation and their high stability constant with DTPA compared to that of the barium cations (Ba^{2+}) as shown in Table 1[38] contribute to producing the barite scale.[36] This occurs when the DTPA drops the barium cation and replaced with the calcium cation.

Table 1. Equilibrium Constant of Different Chelating Agents with the Different Metallic Ions[38]

chelating agents	metallic ion	log K_{MY}
DTPA	Ca	10.34
	Mg	8.92
	Ba	8.87
EDTA	Ca	10.59
	Mg	8.69
	Ba	7.76

A similar mechanism is expected in solution (ii) when EDTA was used as a removal solution. The difference lies in the stability constant of EDTA with Ca^{2+} and Ba^{2+}, which will affect the secondary damage percentage. For the proposed solution (iii) in this study, the usage of both DTPA and EDTA at the same time can limit the secondary damage. As can be seen in Table 1, the stability constant of DTPA with Ba^{2+} cations is higher compared to the stability constant of EDTA with the same cations. This reflects the impact for the brine as well, where different ions will have different impacts based on the stability constant. On the same note for the investigated ions, EDTA has higher stability than DTPA with Ca^{2+} cations. First, they encounter the barite filter cake where the Ba^{2+} cation is abundant; both will chelate the barium cation with a higher degree of DTPA attachment compared to that of EDTA due to the difference in the stability constant. In this step (c), there will be DTPA, EDTA, Ba-DTPA, and Ba-EDTA in the solution based on the availability of barium cations. When they come in contact with the formation, it is more favorable for EDTA to complex with Ca^{2+} cations compared to Ba^{2+} cations and vice versa for DTPA to chelate Ba^{2+} cations compared to Ca^{2+} cations. This will act as an inhibition mechanism to minimize the barite scale formation.

2.1. Rock Sample. Two carbonate core rock samples were used in this study, which are known as Indiana carbonate. The permeability and porosity values of the rock core plugs used in this study are listed in Table 2. Both core plugs were saturated using brine (3% KCl) to measure the liquid permeability and then vacuumed and saturated with sodium sulfate ($NaSO_4$). Gas porosity and permeability were measured using an automated permeameter−porosimeter (AP-608) from Coretest system Inc. The AP-608 instrument applies Boyle's law to measure the porosity and pulse decay with the Klinkenberg effect to measure gas permeability.

Table 2. Core Sample Properties

sample ID	helium permeability (mD)	liquid permeability (mD)	porosity (%)
1	170	64	15.5
2	176	97	16.1

2.2. Materials. Industrial grade barite was used in this study with particle size less than 75 μm, which was obtained by sieving the barite particles. Diethylenetriamine pentaacetic acid potassium-based (K_5-DTPA) and ethylenediamine tetraacetic acid potassium-based (K_4-EDTA) were utilized with a concentration of 20% and a pH of 12. Both solutions were prepared using the potassium base, which is stated as the optimum base for barite dissolution.[28]

2.3. Experimental Apparatus and Procedures. This subsection will present the main apparatus and procedures used in this work with a detailed methodology for each test. The tests include particle size analysis, scanning electron microscopy (SEM), X-ray diffraction (XRD), core flooding test, NMR measurements, solubility test, and inductively coupled plasma mass spectrometry (ICP spectroscopy).

2.3.1. Particle Size Distribution (PSD). The industrial barite was analyzed using the ANALYSETTE 22 Nano Tec plus unit to obtain the particle size distribution.

2.3.2. Scanning Electron Microscopy (SEM). Scanning electron microscopy (SEM-EDS) was utilized to determine the chemical composition of the industrial barite. Several spots were imaged to study the distribution of the chemical composition among the samples to evaluate the purity of the industrial grade barite before the core flooding test. Moreover, the high-resolution images of SEM were acquired to visualize the surface area of the barite particles.

2.3.3. X-Ray Diffraction (XRD). The mineralogy of the barite was identified using the PANalytical X-ray, Philips analytical equipment. The XRD results can serve as a confirmation of the SEM results. It provides the characterization and identification of the mineralogical composition of the sample. XRD is where an X-ray encounters different planes of a crystal lattice. Hence, each peak can be used as a signature for a specific mineral.

https://doi.org/10.1021/acsomega.2c01339
ACS Omega 2022, 7, 17976−17983

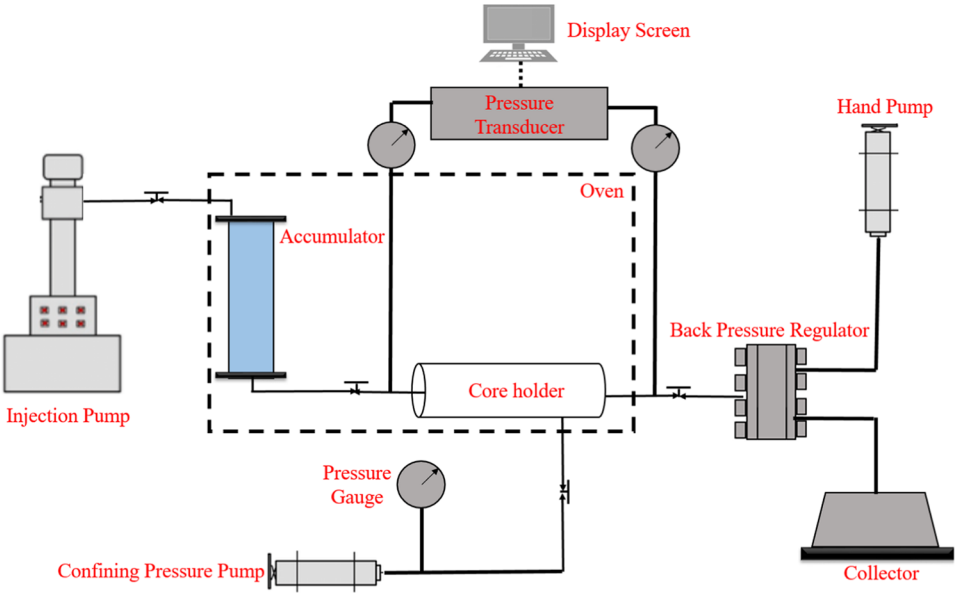

Figure 2. Core flooding Schematic Diagram.

2.3.4. Core Flooding Test. The used core flooding system as shown in Figure 2 in this work consists of a heating oven to control the temperature, injection pump to pump the fluid inside the core, overburden pressure pump and backpressure regulator to control the pressure, accumulator to store the fluids, core holder to hold the core inside the system, sample collector to accumulate the effluent, and data acquisition and recording system to, respectively, monitor and record important parameters such as injection rate, pressure, and temperature.

The system temperature was elevated gradually until it reached 212 °F, and to allow the distribution of temperature uniformly throughout the core and the accumulators, the system was kept for 4 h before injection for temperature stabilization. The permeability was measured using four different injection rates namely 0.5, 1.0 1.5, and 2.0 cm^3/min at a single-phase and steady-state flow of KCl brine. Darcy's single-phase equation was applied to estimate the liquid permeability.

After the permeability measurement, two pore volumes (PV) of the solution (DTPA saturated with barium and EDTA) were injected into the cores at an injection rate of 0.25 cc/min. The backpressure was set to 1000 psi at the end of the core to guarantee a constant pore pressure of 1000 psi. Both inlet and outlet valves were closed after the injection for 18 h to ensure that the reaction takes place. The cores were then flushed with brine, and the permeabilities were measured again after the aging process.

2.3.5. Nuclear Magnetic Resonance (NMR). The measurement of T_2 relaxation time was performed using a Geospec 2.1 rock analyzer from Oxford Instruments (low magnetic field NMR (2 MHz)). The measurements were done at two different stages: after saturating the cores with 3 wt % KCl brine and after the core flooding test. The CPMG pulse sequence was utilized with the following optimization parameters: Tau value of 0.1 ms; signal to noise ratio of 200; and recycle delay of 11 250 ms. The inversion of the raw CPMG data was analyzed using Tikhonov regularization, which uses a non-negative least squares algorithm.[39] The regularization coefficients were chosen to optimize the goodness of fit.

2.3.6. Solubility Test. Industrial grade barite particles were placed in a flask containing the K_5-DTPA solution, and it was soaked for 24 h at an elevated temperature of 270 °F. The maximum limit of barite solubility in the K_5-DTPA solution is found to be 36 g/L.[28] After that, K_4-EDTA was added to the solution with a concentration of 20%. Calcium carbonate ($CaCO_3$) was added gradually to the solution while stirring at a temperature of 176 °F. The calcium and barium concentrations were traced with time using ICP spectroscopy. The solution at the end of the experiment was then filtrated using 2 micron filter paper, and the participated solids were tested using HCl acid.

2.3.7. ICP Spectroscopy Test. The ICP spectroscopy test was performed for each sample taken from the solubility test to identify the concentrations of barium and calcium in the solution. Whenever needed, the dilution process of samples was performed to meet the ICP spectroscopy detection range.

3. RESULTS AND DISCUSSION

3.1. Industrial Barite Characterization. The particle distribution size of the barite used in this work is shown in Figure 3. The results show that the majority of the barite particles fall in the range of 30−40 μm.

Three different spots in the barite samples were chosen using SEM-EDS to characterize the elemental composition. The SEM results, listed in Table 3, showed the composition analysis for the barite particles for the three different sample spots to obtain representative data. Based on the acquired data, the most dominant elements in barite (i.e., $BaSO_4$) are barium (Ba), sulfur (S), and oxygen (O), which represent a total of more than 94% of the composition. The impurities in the used barite sample are silicon (Si), aluminum (Al), iron (Fe), calcium (Ca), and potassium (K), which represent almost 6% of the composition. In addition, the high-resolution images obtained by SEM are shown at 5 μm resolutions in Figure 4. One particle of the barite is shown in the high-resolution image (i.e., 5 μm), and it shows that the pore size of the sample is in the range of 2−3 μm in length and 1−2 μm in width. Figure 5

https://doi.org/10.1021/acsomega.2c01339
ACS Omega 2022, 7, 17976−17983

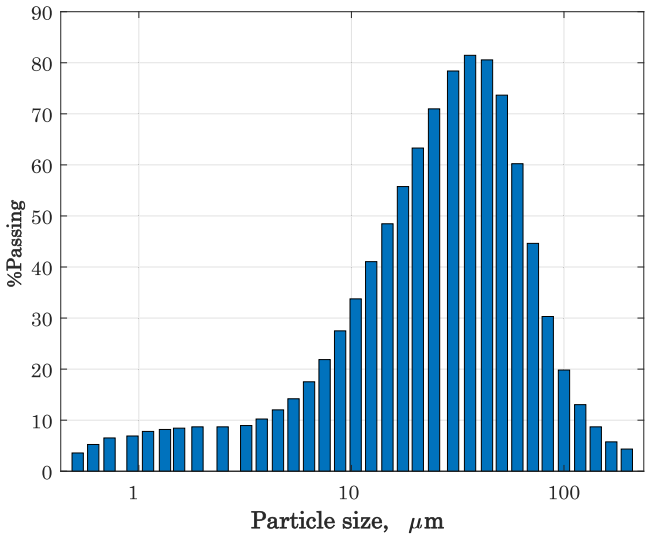

Figure 3. Barite particle size distribution.

Table 3. Composition Analysis for the Industrial Barite

element	spectrum 1 (wt %)	spectrum 2 (wt %)	spectrum 3 (wt %)
Ba	56.34	54.97	56.11
O	26.23	27.54	25.97
S	11.67	11.88	11.96
Si	3.53	3.46	3.65
Al	0.92	0.89	0.94
Fe	0.54	0.55	0.56
Ca	0.44	0.41	0.47
K	0.33	0.3	0.34

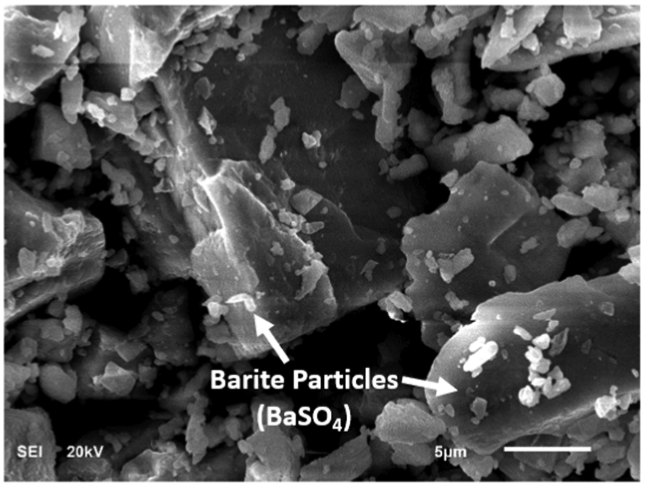

Figure 4. SEM image of the barite particles at 5 μm.

confirms that the purity of the barite was almost 95%; the unknown peaks represent the impurities in the sample.

3.2. Evaluation of Rock Stimulation. In previous study,[36] it was found that due to the existence of a high amount of calcium ions in carbonate formations, the chelating agent solution (K_5-DTPA saturated with barium) tends to precipitate in the surface of the formation. The presented NMR results for the carbonate core sample showed that the macropores were blocked due to barite precipitation. Meanwhile, the chelating agent became active after dropping the loaded barium and dissolved the Ca^{2+} ions, so the micropores were enlarged. This phenomenon was attributed to the abundance and the existence of suitable ions to induce the ion exchange. The opposite occurred in previous study for sandstones where barite precipitation happens in the micropores (sites of the metallic ions).[36]

In this work, 20% of K_4-EDTA was added to the saturated K_5-DTPA with barium to decrease the precipitation of barium in the macropores of calcite formations. Figures 6 and 7 show the T_2 relaxation time distribution before and after the interaction with the barite-saturated chelating agent for samples 1 and 2, respectively. The black curve shows the T_2 relaxation time distribution before the flooding with the two-pore system (i.e., dual porosity) represented by the micro- and macropores. The T_2 relaxation time peak values for the micro- and macropores are given as vertical dashed and dotted lines, respectively. For sample 1, the NMR porosity has increased by 14.73% where it showed 15.61 p.u. before flooding and 17.91 p.u. after flooding. This increase reflected its implication in the pore size distribution as shown in the T_2 relaxation distribution in Figure 6. The micropore T_2 relaxation time peak value in sample 1 before flooding was 0.067 ms, and it shifted to a higher relaxation time peak value at 0.160 ms after flooding. Furthermore, the macropore T_2 relaxation time peak value was 0.762 ms before flooding and moved to a higher relaxation time at 1.091 ms after flooding. A plausible explanation for the T_2 distribution shift to higher relaxation components is the pore size enlargement. After the core flooding experiment, the micropores were enlarged due to the presence of EDTA. This could be justified that EDTA reacted with calcite and DTPA was not capable of dropping the barium in the macropores. The precipitation occurred in the smaller pores for both samples. Even though there is quite a little precipitation in the macropores, they were also stimulated, which have a major contribution to the flow compared to that of the micropores. The T_2 relaxation distribution of sample 2 as shown in Figure 7 emphasizes the same behavior for sample 1 with a 10.97% percentage increase in NMR porosity (from 16.41 to 18.21 p.u.). Moreover, the T_2 relaxation time peak value of the micropores increased from 0.065 to 0.123 ms, while it increased in the macropores from 0.776 to 0.886 ms in sample 2 as shown in Figure 7.

The liquid permeability and porosity of the core sample before and after the interactions could serve as additional evidence of the efficiency of the solution used in this study. The liquid permeability improved from 64 to 120 mD (87.5% increase) for rock core 1 and increased from 97 to 136.14 mD (40.35% increase) for rock core 2. The incremental improvement in the porosity for both cores was estimated to be 4.5 porosity units.

3.3. Reaction Kinetics of the Proposed Solution. This phenomenon can be attributed to the ions exchanged and the reactive ability of the solution (i.e., K_5-DTPA and K_4-EDTA). Due to the capillary pressure, the flow starts at the big pores with reactive capacity, and it will stimulate the micropores when it is in contact for a sufficient time with the surface. As the flow continues, it proceeds to invade the smaller pores with barium-laden and calcium-laden saturated chelating agents. The availability of different ions with affinity of the chelate to them induces an ion exchange process between the chelating agents and the other ions. This leads to some precipitation (i.e., barium sulfate) in the micropores, which was confirmed from the NMR T_2 relaxation distribution. The existence of small microfractures in the second sample caused the process

https://doi.org/10.1021/acsomega.2c01339
ACS Omega 2022, 7, 17976−17983

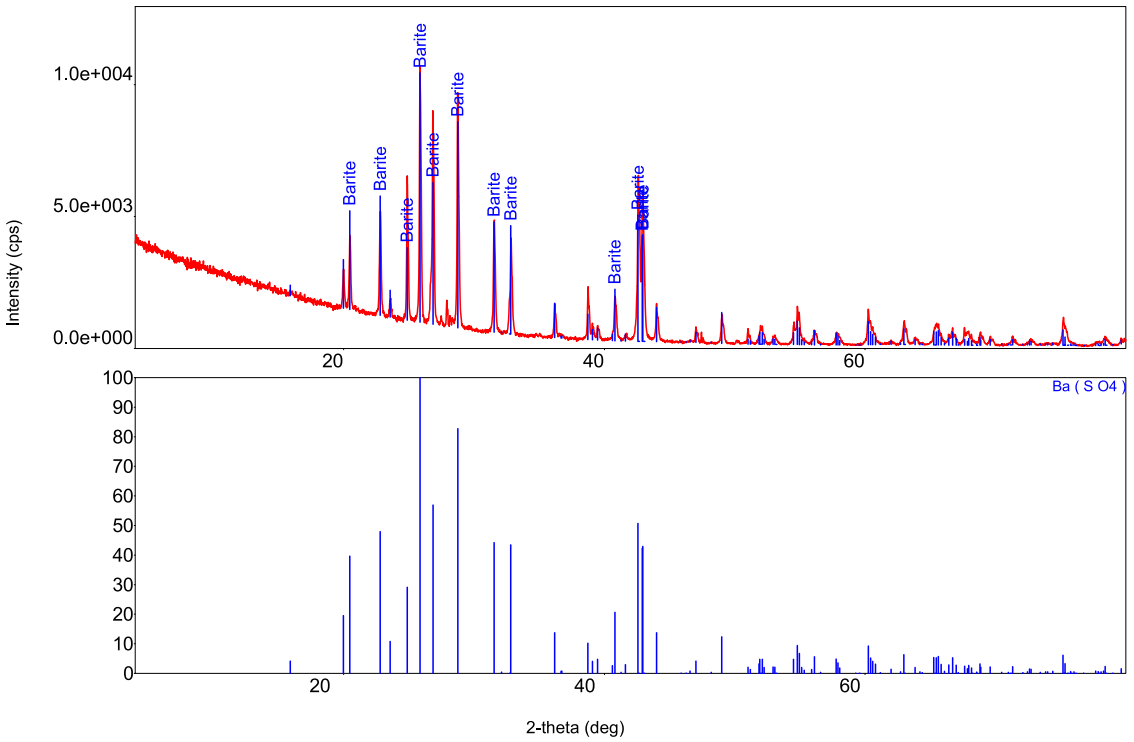

Figure 5. Mineral composition of barite (XRD).

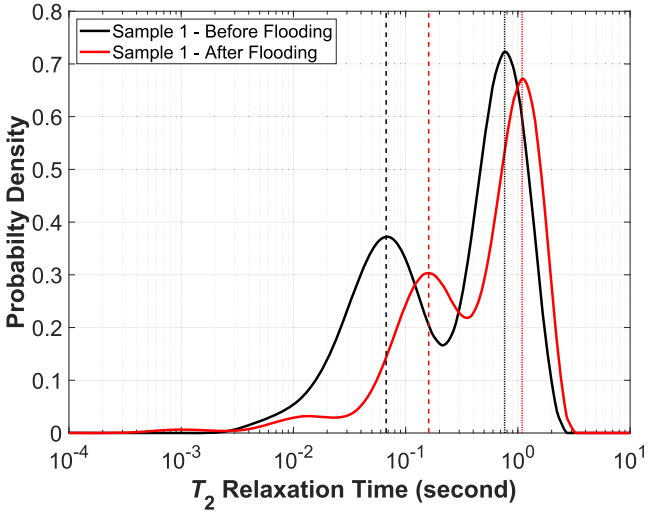

Figure 6. T_2 relaxation time distribution for sample 1 before and after the core flooding.

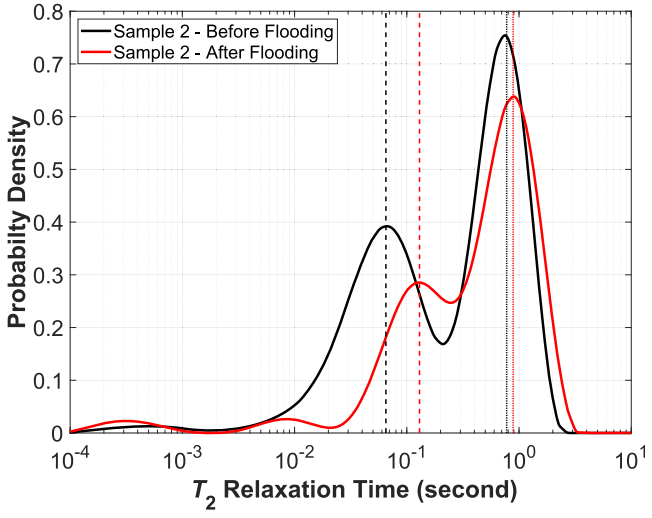

Figure 7. T_2 relaxation time distribution for sample 2 before and after the core flooding.

to continue, and the chelating agents were able to enlarge them.

The solubility test shows the effect of the calcium ions on the barium-saturated chelating agents with time. As shown in Figure 8, the solution was able to dissolve both barium sulfate and calcium carbonate without and with precipitation up to 36 and 42 g/L for barite and calcium carbonate, respectively. After that, any addition amount of calcium carbonate in the solution will affect the dissolution of the barite in the solvent (DTPA) and caused the drop of barium as barite with immediate replacement of Ba^{+2} with Ca^{+2}. To confirm that the precipitated solids are barite, the solution was filtrated with 2 micron filter paper, and then, the solids were dried using an oven at 120 °C. After that, the solids were subjected to HCl treatment, and they showed zero solubility in HCl, which confirmed that the dropped particles in the solution are barite since calcium carbonate reacts with the acid.[40] This replacement process can be explained by the preference of each chelating agent to be stable, so it attached itself with the metallic ions with a higher equilibrium constant as shown previously in Table 1. In other words, it can be concluded that the proposed solution consisting of a mixture of both DTPA and EDTA was able to load 35 000 ppm barium in the presence of calcite ions. The addition of EDTA tends to inhabit the barite deposition until the concentration of calcite reached the maximum capability at 43 000 ppm as shown in Figure 6. An additional advantage of the proposed solution is that to reach the maximum allowance amount of calcite

https://doi.org/10.1021/acsomega.2c01339
ACS Omega 2022, 7, 17976−17983

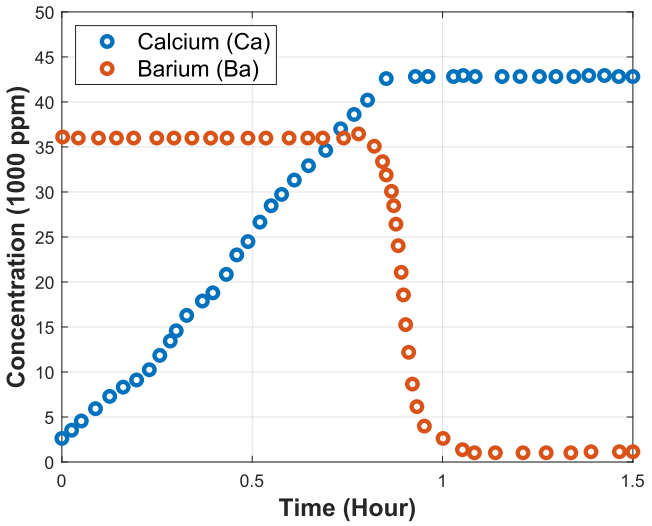

Figure 8. Concentration of barium and calcium in the solution of K_5-DTPA and K_5-EDTA.

concentration, it takes about 1 h. This time was observed in the solubility test where the calcite particles were added as a powder, so the surface area of the reaction is massive. In fact, this would take longer as the calcite and solution will be contacted only on a small area inside the formation.

4. CONCLUSIONS

Secondary damage after the filter cake removal, caused by dropping the barite inside the calcite pores, is a serious problem that needs to be minimized. A solution has been proposed in this study by utilizing a mixture of 20% wt. K_5-DTPA and 20% wt. K_4-EDTA. The following conclusions can be drawn from this study:

- The proposed solution of 20%-K_5-DTPA and 20%-K_5-EDTA shows very promising results to solve the problem of barite scales. It shows the ability of this solution to prevent the precipitation of the barite after the interaction with the carbonate rock core.
- A major advantage of the proposed solution is that it stimulates and enlarges the micropores, which was validated by the NMR T_2 relaxation distribution, while the precipitation of the barite occurred mainly in the macropores.
- The mixture of DTPA and EDTA solutions showed a potential capability to load 35 000 ppm barium in the presence of the calcite ions. The addition of EDTA in the DTPA solution tends to prevent the barite deposition until the concentration of calcite reached the maximum capability at 43 000 ppm.

Table A1. Full Names of the Chelating Agents

chelating agent abbreviations	full names of the chelating agents
DTPA	diethylenetriamine pentaacetic acid
EDTA	ethylenediamine tetraacetic acid
HEDTA	hydroxyethyl ethylenediamine triacetic acid
DOCTA	dioxaocta methylenedinitrilo tetraacetic acid
NTA	nitrile triacetic
TTHA	triethylene tetraamine hexaacetic acid
EDTPO	ethylenediamine tetra(methylenephosphonic) acid

APPENDIX

Table A1

AUTHOR INFORMATION

Corresponding Author

Badr Bageri − *Center for Integrative Petroleum Research, King Fahd University of Petroleum & Minerals, 31261 Dhahran, Saudi Arabia;* orcid.org/0000-0002-7510-0933; Email: badr.bageri@kfupm.edu.sa

Authors

Jaber Al Jaberi − *Department of Petroleum Engineering, King Fahd University of Petroleum & Minerals, 31261 Dhahran, Saudi Arabia*

Abdulmalek Ahmed − *Department of Petroleum Engineering, King Fahd University of Petroleum & Minerals, 31261 Dhahran, Saudi Arabia*

Mahmoud Elsayed − *Department of Petroleum Engineering, King Fahd University of Petroleum & Minerals, 31261 Dhahran, Saudi Arabia*

Mohamed Mahmoud − *Department of Petroleum Engineering, King Fahd University of Petroleum & Minerals, 31261 Dhahran, Saudi Arabia;* orcid.org/0000-0002-4395-9567

Shirish Patil − *Department of Petroleum Engineering, King Fahd University of Petroleum & Minerals, 31261 Dhahran, Saudi Arabia;* orcid.org/0000-0002-0131-4912

Karem Al-Garadi − *Department of Petroleum Engineering, King Fahd University of Petroleum & Minerals, 31261 Dhahran, Saudi Arabia*

Assad Barri − *Department of Petroleum Engineering, King Fahd University of Petroleum & Minerals, 31261 Dhahran, Saudi Arabia*

Complete contact information is available at: https://pubs.acs.org/10.1021/acsomega.2c01339

Author Contributions

The article was written through the contributions of all authors. All authors have approved the final version of the article.

Notes

The authors declare no competing financial interest.

REFERENCES

(1) Lide, D. R. *CRC Handbook of Chemistry and Physics*; CRC Press, London, 2010.

(2) Kresse, R.; Baudis, U.; H, P. J.; Riechers, H.; Wagner, H.; Winkler, J.; Wolf, H. U. Barium and Barium Compounds. *Ullmann's Encycl. Ind. Chem.* **2000**, *4*, 621−640.

(3) Mahmoud, M. A.; Elkatatny, S. Removal of Barite-Scale and Barite-Weighted Water- Or Oil-Based-Drilling-Fluid Residue in a Single Stage. *SPE Drill. Completion* **2019**, *34*, 16−26.

(4) Bageri, B. S.; Adebayo, A. R.; Al Jaberi, J.; Patil, S. Effect of Perlite Particles on the Filtration Properties of High-Density Barite Weighted Water-Based Drilling Fluid. *Powder Technol.* **2020**, *360*, 1157−1166.

(5) Hamad, B. A.; He, M.; Xu, M.; Liu, W.; Mpelwa, M.; Tang, S.; Jin, L.; Song, J. A Novel Amphoteric Polymer as a Rheology Enhancer and Fluid-Loss Control Agent for Water-Based Drilling Muds at Elevated Temperatures. *ACS Omega* **2020**, *5*, 8483−8495.

(6) Magzoub, M. I.; Salehi, S.; Hussein, I. A.; Nasser, M. S. Investigation of Filter Cake Evolution in Carbonate Formation Using Polymer-Based Drilling Fluid. *ACS Omega* **2021**, *6*, 6231−6239.

https://doi.org/10.1021/acsomega.2c01339
ACS Omega 2022, 7, 17976−17983

(7) Mahmoud, M.; Bageri, B. S.; Elkatatny, S.; Al-Mutairi, S. H. Modeling of Filter Cake Composition in Maximum Reservoir Contact and Extended Reach Horizontal Wells in Sandstone Reservoirs. *J. Energy Resour. Technol.* **2017**, *139*, No. 032904.
(8) Hartmann, A.; Ozerler, M.; Marx, C.; Neumann, H.-J. Analysis of Mudcake Structures Formed Under Simulated Borehole Conditions. *SPE Drill. Completion* **1988**, *3*, 395−402.
(9) Chenevert, M. E.; Huycke, J. Filter Cake Structure Analysis Using the Scanning Electron Microscope. *Society of Petroleum Engineers*, SPE 22208, 1991.
(10) Bageri, B. S.; Mahmoud, M. A.; Sultan, A. S. S.; Al-Mutairi, S. H.; Abdulraheem, A. In *Effect of the Drilled Cuttings on Filter Cake Sealing Properties and Internal Invasion Depth in MRC Wells*, Oil Gas Show Conference SPE-175168, Mishref, Kuwait, Oct 11−14, 2015.
(11) Bageri, B. S.; Mahmoud, M. A.; Al-Mutairi, S. H.; Abdulraheem, A. In *Filter Cake Porosity and Permeability Profile Along the Horizontal Well and Their Impact on Filter Cake Removal*, International Petroleum Technology Conference, IPTC-18465-MS, Doha, Qatar, Dec 6−9, 2015.
(12) Bageri, B. S.; Mahmoud, M.; Al-Mutairi, S. H.; Abdulraheem, A. Effect of Sand Content on the Filter Cake Properties and Removal During Drilling Maximum Reservoir Contact Wells in Sandstone Reservoir. *J. Energy Resour. Technol.* **2016**, *138*, No. 032901.
(13) Bageri, B. S.; Benaafi, M.; Mahmoud, M.; Patil, S.; Mohamed, A.; Elkatatny, S. Effect of Arenite, Calcareous, Argillaceous, and Ferruginous Sandstone Cuttings on Filter Cake and Drilling Fluid Properties in Horizontal Wells. *Geofluids* **2019**, *2019*, No. 1956715.
(14) Hossain, M. E.; Al-Majed, A. A. *Fundamentals of Sustainable Drilling Engineering*, 2015, DOI: 10.1002/9781119100300.
(15) Gamal, H.; Bageri, B. S.; Elkatatny, S.; Patil, S. Investigating the Alteration of Sandstone Pore System and Rock Features by Role of Weighting Materials. *ACS Omega* **2021**, *6*, 4100−4110.
(16) Dreher, T.; Biley, A.; Tuckett, P. In *Stop Erosion at the Well Head on Fractured Wells*, Proceedings of the Annual Offshore Technology Conference, 2014; Vol. 1, pp 483−487.
(17) Al Jaber, J.; Bageri, B. S.; Gamal, H.; Elkatatny, S. The Role of Drilled Formation in Filter Cake Properties Utilizing Different Weighting Materials. *ACS Omega* **2021**, *6*, 24039−24050.
(18) Bageri, B. S.; Mahmoud, M. A.; Shawabkeh, R. A.; Al-Mutairi, S. H.; Abdulraheem, A. Toward a Complete Removal of Barite (Barium Sulfate BaSO 4) Scale Using Chelating Agents and Catalysts. *Arabian J. Sci. Eng.* **2017**, *42*, 1667−1674.
(19) Nasr-El-Din, H. A.; Al-Mutairi, S. H.; Al-Hajji, H. H.; Lynn, J. D. In *Evaluation of a New Barite Dissolver: Lab Studies*, SPE 86501, Present. SPE International Symposium and Exhibition on Formation Damage Control Feb 18−20, 2004.
(20) Mazoyer, P.; Geantet, C.; Diehl, F.; Loridant, S.; Lacroix, M. Role of Chelating Agent on the Oxidic State of Hydrotreating Catalysts. *Catal. Today* **2008**, *130*, 75−79.
(21) Cheng, Y.; Chen, R.; Wang, P.; Wang, Q.; Wan, S.; Huang, S.; Su, R.; Song, Y.; Yang, X.; Fu, X. Synthesis of a Novel Biochar-Supported Polycarboxylic Acid-Functionalized Nanoiron Oxide-Encapsulated Composite for Wastewater Treatment: Removal of Cd(II), EDTA and Cd-EDTA. *J. Mater. Sci.* **2021**, *56*, 18031−18049.
(22) Lim, T.-T.; Tay, J.-H.; Wang, J.-Y. Chelating-Agent-Enhanced Heavy Metal Extraction from a Contaminated Acidic Soil. *J. Environ. Eng.* **2004**, *130*, 59−66.
(23) Xi, J.; Zhang, L.; Zheng, W.; Zeng, Q.; He, Y.; He, Z.; Chen, J. Anchoring DTPA Grafted PEI onto Carboxylated Graphene Oxide to Effectively Remove Both Heavy Metal Ions and Dyes from Wastewater with Robust Stability. *J. Mater. Sci.* **2021**, *56*, 18061−18077.
(24) Barri, A.; Hassan, A.; Mahmoud, M. Carbonate Stimulation Using Chelating Agents: Improving the Treatment Performance by Optimizing the Fluid Properties. *ACS Omega* **2022**, *7*, 8938−8949.
(25) Lakatos, I.; Lakatos-Szabó, J.; Kosztin, B. Optimization of Barite Dissolvers by Organic Acids and PH Regulation In *SPE Oilfield Scale Symposium*, 2002; pp 147−156.
(26) Lakatos, I.; Lakatos-Szabó, J.; Kosztin, B. In *Comparative Study of Different Barite Dissolvers: Technical and Economic Aspects*, SPE International Symposium and Exhibition on Formation Damage Control, Society of Petroleum Engineers, 2002.
(27) Mahmoud, M. Removing of Formation Damage and Enhancement of Formation Productivity Using Environmentally Friendly Chemicals, Texas A&M, 2011.
(28) Bageri, B. S.; Mahmoud, M. A.; Shawabkeh, R. A.; Abdulraheem, A. Evaluation of Barium Sulfate (Barite) Solubility Using Different Chelating Agents at a High Temperature. *J. Pet. Sci. Technol.* **2017**, *7*, 42−56.
(29) Bageri, B. S.; Mahmoud, M. A.; Al-Majed, A. A.; Al-Mutairi, S. H.; Abdulazeez, A.; Shawabkeh, R. In *Water Base Barite Filter Cake Removal Using Non-Corrosive Agents*, SPE Middle East Oil and Gas Show and Conference, MEOS, SPE-183653-MS, Manama, Kingdom of Bahrain, March 6−9, 2017; pp 2940−2947.
(30) Bageri, B. S.; Mahmoud, M.; Abdulraheem, A.; Al-Mutairi, S. H.; Elkatatny, S. M.; Shawabkeh, R. A. Single Stage Filter Cake Removal of Barite Weighted Water Based Drilling Fluid. *J. Pet. Sci. Eng.* **2017**, *149*, 476−484.
(31) Mahmoud, M. A.; Bageri, B. S.; Abdelgawad, K.; Kamal, S. M.; Hussein, I.; Elkatantny, S.; Shawabkeh, R. Evaluation of the Reaction Kinetics of Diethylenetriaminepentaacetic Acid Chelating Agent and a Converter with Barium Sulfate (Barite) Using a Rotating Disk Apparatus. *Energy Fuels* **2018**, *32*, 9813−9821.
(32) Vetter, O. J. G. How Barium Sulfate Is Formed: An Interpretation. *J. Pet. Technol.* **1975**, *27*, 1515−1524.
(33) Bageri, B. S.; Adebayo, A. R.; Barri, A.; Al Jaberi, J.; Patil, S.; Hussaini, S. R.; Babu, R. S. Evaluation of Secondary Formation Damage Caused by the Interaction of Chelated Barite with Formation Rocks during Filter Cake Removal. *J. Pet. Sci. Eng.* **2019**, *183*, No. 106395.
(34) Al Jaberi, J.; Bageri, B. S.; Barri, A.; Adebayo, A.; Patil, S.; Babu, R.; Rizwanullah, S. In *Insight into Secondary Posterior Formation Damage During Barite Filter Cake Removal in Calcite Formations*, International Petroleum Technology Conference held in Dharan, Saudi Arabia, IPTC-19611, January, 2020.
(35) Abdelgawad, K.; Mahmoud, M.; Elkatatny, S.; Patil, S. In *Effect of Calcium Carbonate on Barite Solubility Using a Chelating Agent and Converter*, Proceedings - SPE International Symposium on Oilfield Chemistry, 2019, Vol. 2019.
(36) Bageri, B. S.; Adebayo, A. R.; Barri, A.; Al Jaberi, J.; Patil, S.; Hussaini, S. R.; Babu, R. S. Evaluation of Secondary Formation Damage Caused by the Interaction of Chelated Barite with Formation Rocks during Filter Cake Removal. *J. Pet. Sci. Eng.* **2019**, *183*, No. 106395.
(37) Putnis, C. V.; Kowacz, M.; Putnis, A. The Mechanism and Kinetics of DTPA-Promoted Dissolution of Barite. *Appl. Geochem.* **2008**, *23*, 2778−2788.
(38) Fredd, C. N.; Fogler, H. S. The Influence of Chelating Agents on the Kinetics of Calcite Dissolution. *J. Colloid Interface Sci.* **1998**, *204*, 187−197.
(39) Tikhonov, A. N. On the Solution of Incorrectly Put Problems and the Regularisation Method. *Outlines Jt. Symp. Partial Differ. Equations* **1963**, *4*, 261−265.
(40) Taylor, K. C.; Al-Ghamdi, A. W. M.; Nasr-El-Din, H. A. Measurement of Acid Reaction Rates of a Deep Dolomitic Gas Reservoir. *J. Can. Pet. Technol.* **2004**, *43*, 49−56.

https://doi.org/10.1021/acsomega.2c01339
ACS Omega 2022, 7, 17976−17983